Accuracy Evaluation of Low-Cost and Professional UAS Orthomosaics for 2D/3D Urban Cadastre Mapping

Allan GOMES, Renato Z. ARAUJO and Francisco H. de OLIVEIRA, Brazil

Key words: Urban Cadastre, UAS, Orthomosaic, Accuracy, Georeferencing.

SUMMARY

The increasing demand for precise and timely geospatial information, particularly for the evolving three-dimensional urban cadastre, has positioned Unmanned Aircraft Systems (UAS) as essential data acquisition tools. This study compares the positional accuracy of orthomosaics generated by a low-cost UAS (DJI Mini 3) and a professional platform (DJI Matrice 350 RTK + P1) for urban cadastre applications. Two photogrammetric workflows were tested: indirect georeferencing with ground control points for the Mini 3 and direct georeferencing with Network RTK for the Matrice. The 5-ha study area was flown at 70 m altitude, and accuracy was evaluated using the Brazilian Cartographic Accuracy Standard (PEC) at 1:1000 scale. The Matrice achieved a finer ground sampling distance (0.84 cm) and lower positional RMS (4.09 cm) but required longer processing time (4 h 47 m). The Mini 3 produced an RMS of 11.02 cm with shorter processing time (32 min). Despite these differences, both orthomosaics met PEC Class A requirements, demonstrating that low-cost UAS with indirect georeferencing can provide a cost-effective alternative for accurate 2D cadastral mapping.

RESUMO

A crescente demanda por informações geoespaciais precisas e oportunas, particularmente para o cadastro urbano tridimensional em evolução, posicionou os Sistemas de Aeronaves Não Tripuladas (UAS) como ferramentas essenciais de aquisição de dados. Este estudo compara a acurácia posicional de ortomosaicos gerados por um UAS de baixo custo (DJI Mini 3) e por uma plataforma profissional (DJI Matrice 350 RTK + P1) para aplicações de cadastro urbano. Foram testados dois fluxos fotogramétricos: georreferenciamento indireto com pontos de controle para o Mini 3 e georreferenciamento direto com Network RTK para o Matrice. A área de estudo (5 ha) foi imageada a 70 m de altitude, e a acurácia foi avaliada pelo Padrão de Exatidão Cartográfica (PEC) na escala 1:1000. O Matrice obteve menor GSD (0,84 cm) e RMS posicional (4,09 cm), mas exigiu maior tempo de processamento (4 h 47 m). O Mini 3 apresentou RMS de 11,02 cm com tempo total de apenas 32 min. Apesar das diferenças, ambos os ortomosaicos atenderam à Classe A do PEC, demonstrando que UAS de baixo custo com georreferenciamento indireto podem ser uma alternativa economicamente viável para mapeamento cadastral 2D de alta precisão.

Accuracy Evaluation of Low-Cost and Professional UAS Orthomosaics for 2D/3D Urban Cadastre Mapping

Allan GOMES, Renato Z. ARAUJO and Francisco H. de OLIVEIRA, Brazil

1. INTRODUCTION

The multipurpose land cadastre, increasingly evolving toward a three-dimensional system, demands precise and timely geospatial information. Unmanned Aircraft Systems (UASs) have emerged as essential tools for rapid acquisition of 3D data, including point clouds, Digital Surface Models (DSM), Digital Terrain Models (DTM), and their derivatives such as orthomosaics. Although DSMs and orthomosaics are 2.5D representations, they remain fundamental for feature delineation, photointerpretation, and as visual support for 3D urban modeling.

Urban cadastre is a critical instrument for planning, territorial management, and decision-making in public policy. Its development relies on the availability of accurate, up-to-date spatial information at appropriate scales, which can be obtained through traditional surveying methods or complemented by remote sensing and aerial photogrammetry. Each approach contributes to cadastral databases, differing in cost, coverage, and level of detail.

Recent years have witnessed the widespread adoption of UAS-based photogrammetry due to technological advances and reduced operational costs. Unlike conventional surveying methods, which are often expensive and require specialized expertise, UAS provide rapid data acquisition, adapt to varying operational conditions, and deliver imagery with sufficient resolution to capture small-scale urban features. Integration with Geographic Information Systems (GIS) further facilitates spatial analysis, 3D modeling, and cadastral updating.

The rapid adoption of UAS in urban cadastre underscores the need to evaluate the quality and cost-effectiveness of available solutions, ranging from low-cost consumer-grade platforms to professional-grade systems equipped with high-precision sensors and advanced GNSS positioning. Assessing whether lower-cost UAS can deliver results compatible with urban cadastre requirements is particularly relevant for smaller municipalities or institutions seeking economically viable solutions.

Accordingly, this study aims to comparatively evaluate the positional accuracy of orthomosaics generated by low-cost and professional-grade UAS, using both direct and indirect georeferencing methods. Visual and geometric aspects are also analyzed to identify potential and limitations of each methodology.

2. THEORETICAL FUNDAMENTALS

2.1 UAS-Based Aerial Photogrammetry

Aerial photogrammetry enables the acquisition of qualitative and quantitative spatial information. High positional accuracy and reliable image interpretation require careful consideration of technical parameters. UAS operation depends on the integration and real-time synchronization of multiple sensors. The Global Navigation Satellite System (GNSS)

provides geodetic coordinates, while the Inertial Measurement Unit (IMU) continuously measures aircraft attitude (pitch, roll, and yaw) and supports autonomous navigation (Blázquez and Colomina, 2012). This integration ensures stable flight and enables pre-planned missions, critical for consistent image acquisition. Although manual flight is possible, photogrammetric applications typically require autonomous execution of pre-defined flight paths to guarantee complete coverage and sufficient image overlap. IMU data compensates for aircraft motion during image capture, and GNSS allows for real-time navigation and precise georeferencing of images at the moment of capture.
Cartographic products are generated using photogrammetric processing workflows, including Bundle Block Adjustment (BBA) and Structure from Motion (SfM) algorithms, which combine positional and attitude data to reconstruct 3D scene geometry (Jiménez-Martínez et al., 2021; Sanz-Ablanedo et al., 2018). Thus, GNSS positioning is indispensable for both navigation and accurate georeferencing. Additional factors affecting photogrammetric accuracy include camera calibration (focal length, principal point, lens distortion), flight parameters (altitude, speed, overlap), atmospheric conditions, and ground control points (GCPs) (Cledat et al., 2020; Štroner et al., 2021). These elements complement GNSS data and are essential when targeting the precision required for urban cadastral applications.

2.2 GNSS Positioning Methods and Georeferencing

GNSS positioning directly affects flight navigation, image georeferencing, and mapping product accuracy. The basic method employed by all UAS platforms is Single Point Positioning (SPP), also called Absolute Positioning, which provides meter-level accuracy using a single receiver. While sufficient for navigation, SPP is inadequate for high-precision cartographic products. Differential methods achieve centimeter- or millimeter-level accuracy. Real-Time Kinematic (RTK) and Network RTK rely on a reference station (Base) transmitting corrections to the moving receiver (Rover). Standard RTK requires a Base near the survey area with radio communication, whereas Network RTK transmits corrections via internet using the NTRIP protocol, eliminating the need for a local Base. Post-Processed Kinematic (PPK) applies corrections after the flight, allowing high precision without real-time connectivity (LEICK et al., 2015). Brazil's Continuous Monitoring Network (RBMC - Rede Brasileira de Monitoramento Contínuo) supports NTRIP and PPK, offering free correction services via registration (IBGE, n.d.). The precision of all differential methods decreases with increasing baseline distance, highlighting the importance of planning for large survey areas.
Georeferencing requires reconstruction of perspective rays using interior orientation parameters (focal length, principal point, lens distortions) and exterior orientation parameters (camera position and attitude) (Mikhail et al., 2001). Indirect georeferencing relies on accurately surveyed ground control points (GCPs) with centimeter-level precision. While highly accurate, indirect georeferencing is time-consuming and may be impractical in areas where GCPs cannot be deployed (forests, water bodies, hazardous zones). The direct georeferencing is achieved via GNSS + IMU integration, providing camera position and attitude without ground targets. This method is advantageous in inaccessible areas but inherits positional accuracy from the GNSS method used.
Modern UAS frequently store geodetic coordinates and aircraft attitude in image metadata at capture. This capability allows direct georeferencing in processing software, accelerating product generation while reducing the dependence on ground control points. Nonetheless,

final accuracy remains contingent on the GNSS method employed, products generated using SPP will carry meter-level uncertainty, while RTK/Network RTK/PPK can deliver centimeter-level precision. Selecting an appropriate GNSS positioning strategy is therefore crucial for high-quality photogrammetric outcomes.

2.3 Accuracy Assessment

The accuracy of georeferencing can be assessed by analyzing the residuals of check points following a BBA or by comparing the coordinates of these points with those derived from photogrammetric products, such as DSM or orthomosaics. Even when direct georeferencing is employed, photo-identifiable check points remain essential to evaluate the positional accuracy of the resulting products.
In Brazil, the accuracy of orthomosaics and other cartographic products is classified according to the Cartographic Accuracy Standard (PEC – Padrão de Exatidão Cartográfica), established by national cartographic regulations (Decree No. 89.817) (BRASIL, 1984). According to this standard, planimetric (horizontal) accuracy is defined based on the map scale denominator (DE), while altimetric (vertical) accuracy is defined in relation to the contour interval (eq). This classification allows maps to be categorized according to their positional accuracy and precision, facilitating objective assessment for urban cadastre and other geospatial applications. Table 1 summarizes the PEC classes, their respective thresholds, and the standard error (EP) allowed for planimetric and altimetric assessments.

Table 1. PEC (BRASIL, 1984).

Planimetric			Altimetric		
Class	PEC (mm x DE)	EP (mm x DE)	Class	PEC	EP
A	0.5	0.3	A	1/2 eq	1/3 eq
B	0.8	0.5	B	3/5 eq	2/5 eq
C	1.0	0.6	C	3/4 eq	1/2 eq

Following the methodology proposed by Merchant, 1982 and applied by Galo and Camargo, 1994, the PEC classification can be verified through statistical analysis of the discrepancies between the measured coordinates of reference check points and those extracted from the cartographic product under evaluation. The GeoPEC software (version 3.6) (Geopec, n.d.) provides a robust framework for evaluating the positional accuracy of cartographic and photogrammetric products according to multiple standards. It supports assessments based on Decree No. 89.817 with ET-CQDG (DEFESA et al., 2016) and aerial survey products under the INCRA Technical Georeferencing Manual (2nd edition, 2022) for rural property georeferencing (INCRA, 2022). The software facilitates project management, data import/export, check point handling, sample size definition, and statistical analysis of positional discrepancies.

3. MATERIAL AND METHODS

3.1 Experimental setup

3.1.1 Study Area

The study was carried out on the IFSC campus in Florianópolis, SC (~5 hectares), characterized by diverse urban features. A total of 38 photo-identifiable points were established and surveyed, with 11 designated as control points and 27 as check points. The study area also contains a GNSS station belonging to the RBMC, identified as RBMC-IFSC, as shown in Figure 1.

Figure 1. Location of the study area at the IFSC campus in Florianópolis-SC, highlighting the distribution of photo-identifiable points and the RBMC-IFSC GNSS station

3.1.2 Equipment and Data Collection

The geodetic coordinates of the ground control and check points were obtained using the Network RTK method (NTRIP–IBGE). Measurements were performed with a Spectra SP60 geodetic receiver connected to the RBMC-IFSC reference station, ensuring an average three-dimensional accuracy of approximately 2.3 cm.

For aerial data acquisition, two different categories of UAS were used in order to compare performance and cost-effectiveness. The first was the DJI Mini 3, a lightweight and low-cost

quadcopter, while the second was the DJI Matrice 350 RTK equipped with the Zenmuse P1 (35 mm) camera, a professional-grade platform designed for high-precision mapping (Figure 2). Both aircraft record geodetic coordinates and attitude information (yaw, pitch, and roll) in the metadata of each captured image.

Figure 2. DJI Matrice 350 RTK and DJI Mini 3

The main technical specifications of these platforms are presented in Table 2.

Table 2. General UAS specification

Specification	**DJI Mini 3**	**DJI Matrice 350 RTK + P1**
Aircraft type - DJI	Consumer	Professional/Enterprise
Dimensions (folded)	148 × 90 × 62 mm	430 × 420 × 430 mm
Takeoff weight	~249 g	~7.27 kg (with P1 camera)
Flight endurance	~38 min	~55 min
Maximum flight distance	~18 km	~20 km
Maximum flight speed	~16 m/s	~23 m/s
Wind resistance	~10.7 m/s	~12 m/s
Camera focal length	6.7 mm	35 mm (Zenmuse P1)
Sensor size	1/1.3” CMOS	Full-frame 35 mm CMOS
Camera resolution	12 MP	45 MP
GNSS method capability	SPP	SPP, RTK, Network RTK and PPK
Estimated price (2025, BR)	~R$ 4,500–6,000	~R$ 140,000–180,000 (with P1 camera)

The flights were carried out on April 30, 2025 under stable meteorological conditions to minimize potential positional errors. Two independent missions were performed, both planned with a flight altitude of 70 m, camera direction -90º (no oblique), lateral and forward overlaps of 70%, and a cruise speed of 4 m/s to ensure adequate image coverage and parallax for photogrammetric processing.

The mission with the DJI Mini 3 resulted in the acquisition of 112 images, while the DJI Matrice 350 RTK equipped with the Zenmuse P1 camera produced a total of 129 images. During the professional-grade flight, the Matrice 350 RTK operated in Network RTK (NTRIP- RBMC-IFSC) mode, achieving an average three-dimensional positional accuracy of approximately 2.3 cm for the geodetic coordinates stored in the image metadata.

3.2 Image Georeferencing and Product Generation

Image georeferencing was performed using Agisoft Metashape (version 2.1.3.18851), which implements SfM algorithms to reconstruct the spatial orientation of images and generate three-dimensional point clouds. Two workflows were applied: indirect georeferencing for images acquired with the DJI Mini 3, and direct georeferencing for images acquired with the Matrice 350 RTK + P1. For accuracy assessment, check points were measured in all images, while in the indirect method, control points were also measured.
During the alignment step, Metashape requires selecting a precision level from five options: minimal, low, medium, high, and ultra-precise. Each dataset was processed through all levels, and the level yielding the lowest RMS residual for the check points was adopted: medium for the Mini 3 and ultra-precise for the Matrice P1. This step determines the initial accuracy of camera positions and orientations, which are critical for subsequent dense reconstruction.
After alignment, a dense point cloud was generated using the ultra-precise mode, which maximizes spatial detail at the expense of higher computational demand. From this dense cloud, DSM and orthomosaics were produced. No prior corrections were applied to the DSM for orthomosaic generation, allowing evaluation of inherent noise, potential distortions, and the overall quality of the photogrammetric products.
The processing was performed on a notebook running Windows 64-bit OS, equipped with 15.91 GB of RAM, an Intel(R) Core (TM) i7-10750H CPU @ 2.60 GHz, and an NVIDIA GeForce RTX 2060 GPU.

4. RESULTS

4.1 General aspects

The difference in processing time and file size for each stage is summarized in Table 3.

Table 3. Processing time and output size for each UAS workflow

Step	Matrice 350 – P1 (Time)	Matrice – P1 (Size)	Mini 3 (Time)	Mini 3 (Size)
Alignment	9 min 11 s	30.63 MB	32 s	6.05 MB
Depth Maps	1 h 26 min	7.32 GB	11 min 11 s	1.09 GB
Point Cloud	2 h 37 min	12.26 GB	16 min 27 s	8.20 GB
DSM	11 min 19 s	3.95 GB	1 min 26 s	564.39 MB
Orthomosaic	24 min 6 s	3.65 GB	3 min 31 s	544.63 MB
Total	4 h 47 min 36 s	27.81 GB	32 min 7 s	10.39 GB

The data in Table 4 reveal a strong contrast in computational demand between the two platforms. Although the Mini 3 required only about 32 minutes to complete the entire workflow, the Matrice 350 RTK + P1 demanded nearly five hours, generating final datasets almost three times larger. This difference reflects the higher sensor resolution of the P1 and the more detailed geometry captured, which increase the density of tie points and the volume of depth information processed. While the longer processing time and larger file sizes imply greater computational requirements and storage needs, they also indicate richer spatial detail and potentially higher geometric accuracy, attributes that can be decisive in applications where metric precision is critical.

In addition to processing time, the measurement of photo-identifiable targets in all possible images must also be considered. In this step, image resolution and visual clarity are crucial to ensure correct identification of the targets. The ground sampling distance (GSD) obtained with the Matrice 350 RTK + P1 was 0.84 cm, significantly smaller than the 2.34 cm achieved with the Mini 3, providing greater visual detail that is essential for accurate 2D interpretation and the textural quality of 3D models.

Figure 3 illustrates some of the photo-identifiable elements used in this study, highlighting the superior image quality achieved with the Matrice system.

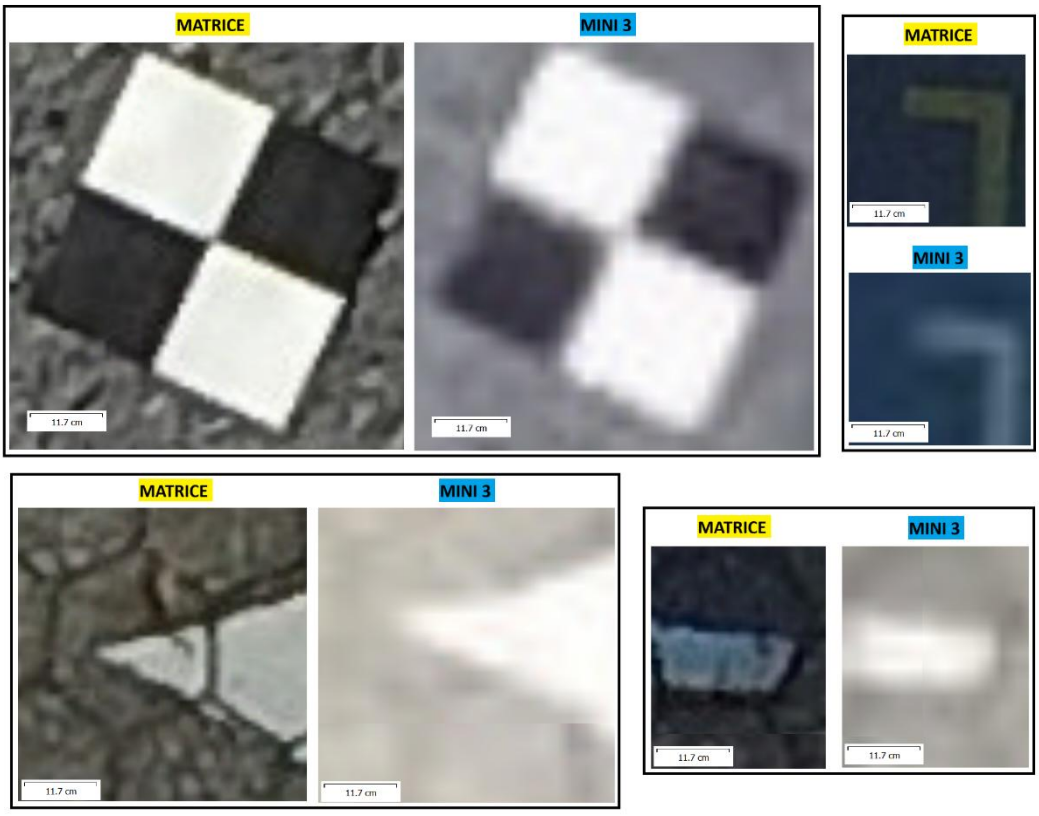

Figure 3. Visual quality of selected photo-identifiable targets

Figure 4 presents the DSMs generated from the two UAS datasets. Although both reconstructions capture the overall campus layout, clear differences in surface fidelity can be observed. The DSM derived from the Mini 3 (top) shows pronounced noise and irregularities, especially in the roof areas of the buildings, which may be attributed to the lower image

resolution. The Matrice 350 + P1 DSM (bottom), in contrast, exhibits more uniform planar surfaces and sharper building outlines, reflecting its finer GSD and higher-quality imagery.
It is important to note that all image acquisitions were performed with a -90° camera angle, whereas for this type of urban scenario the inclusion of oblique imagery is generally recommended to improve the reconstruction of vertical structures and complex roof geometries.

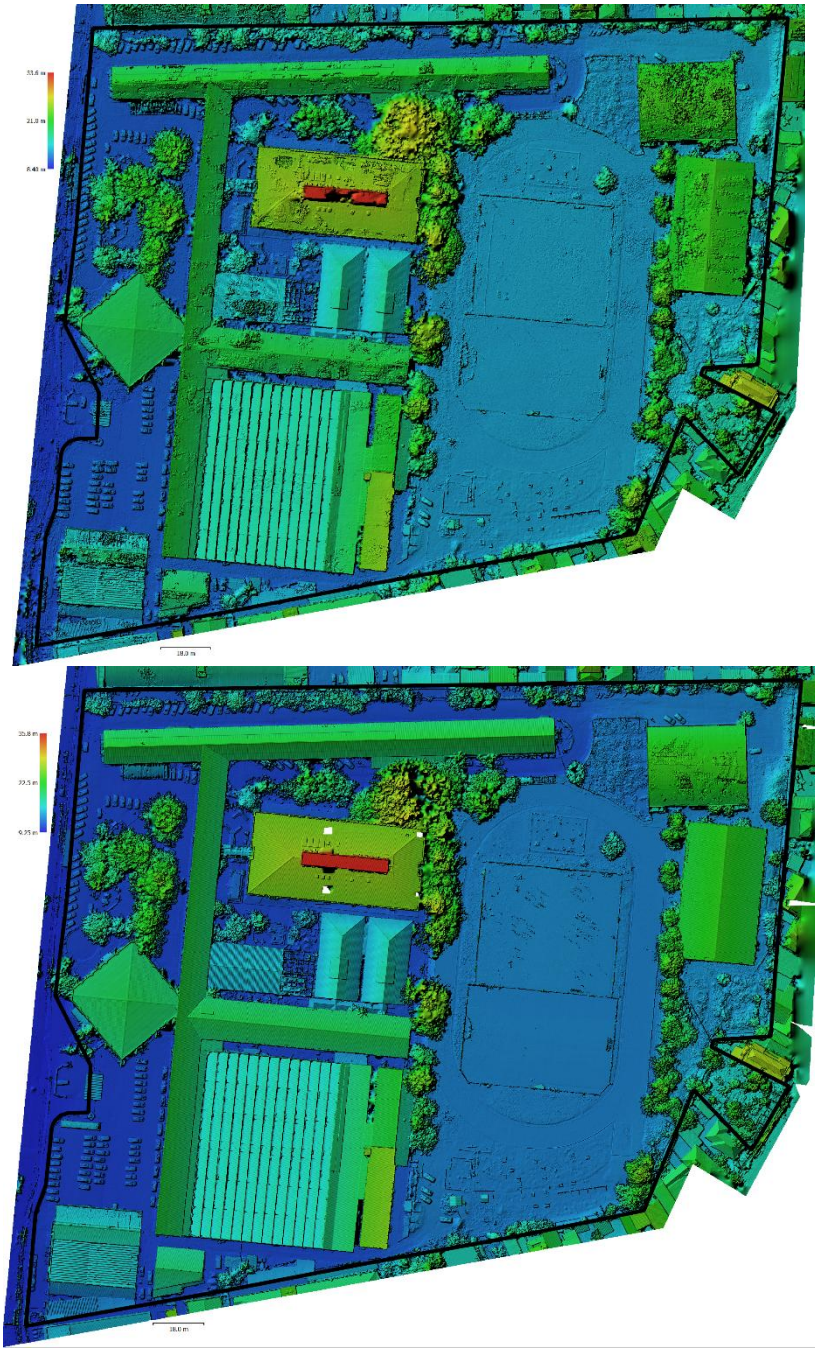

Figure 4. DSMs of the study area generated with the Mini 3 (top) and Matrice 350 + P1 (bottom).

Nevertheless, even in this dataset certain complex structures, such as the circular gymnasium roof in the upper right corner, reveal minor artifacts and slight elevation inconsistencies, highlighting the inherent challenges of modeling curved or highly reflective surfaces. To better illustrate these differences, the next figures present close-up comparisons of selected areas, allowing a more detailed visual inspection of the textural quality and structural definition achieved by each platform. No corrections were applied to the generated DSMs, although such post-processing is available in the software.

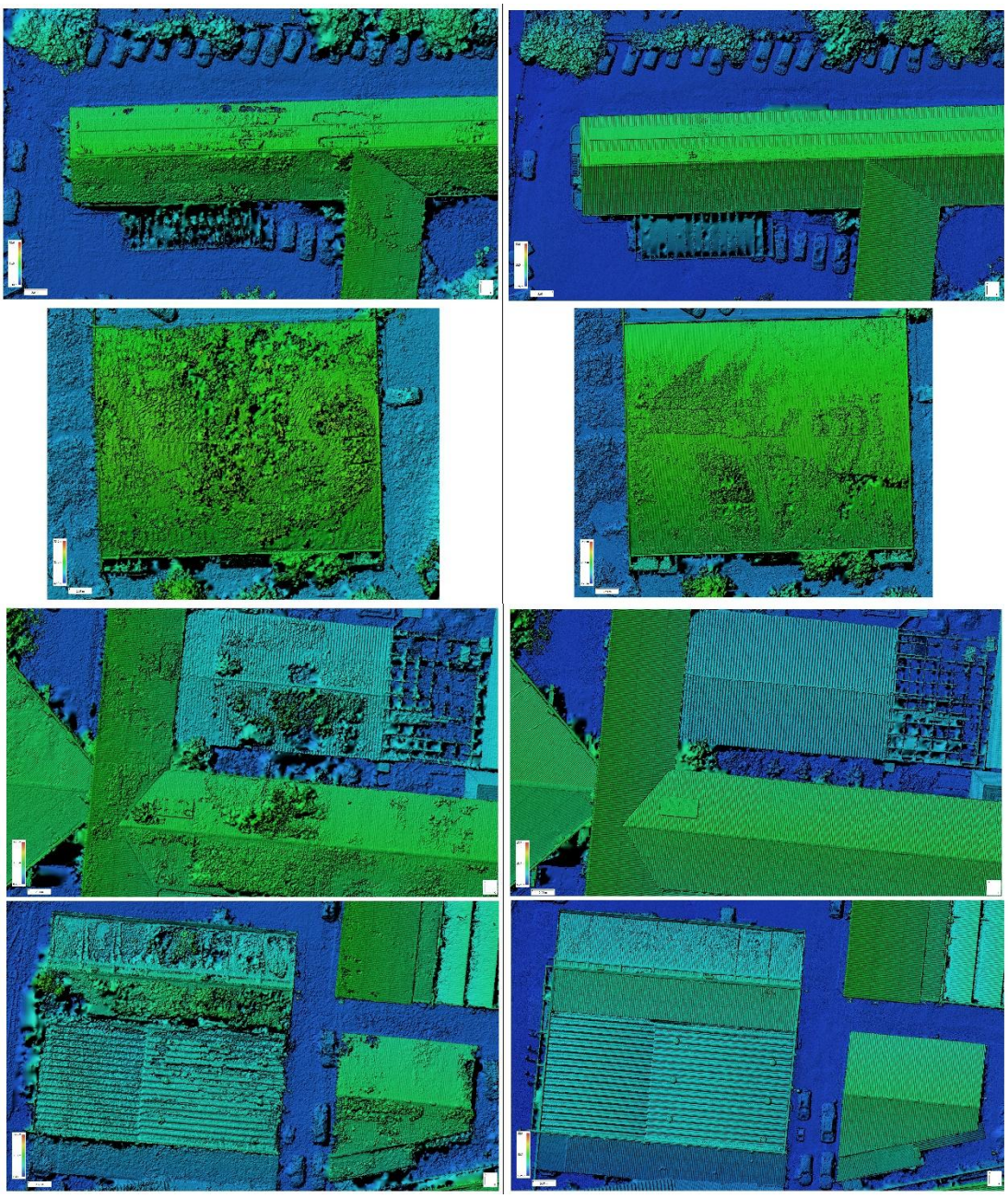

Figure 5. Additional DSM excerpts comparing Mini 3 (left) and Matrice 350 + P1 (right).

Similar to the DSM comparison, Figures 6 and 7 present the two orthomosaics and selected areas highlighted for a more detailed visual inspection. Although the Mini 3 orthomosaic exhibits more residual artifacts and slight misalignments, some discrepancies are also noticeable in the Matrice 350 + P1 product, particularly along building edges, where complex roof geometry and shadowing may introduce local distortions. These observations reinforce that, despite the overall superior quality of the professional-grade platform, post-processing and careful quality control remain necessary for both datasets.

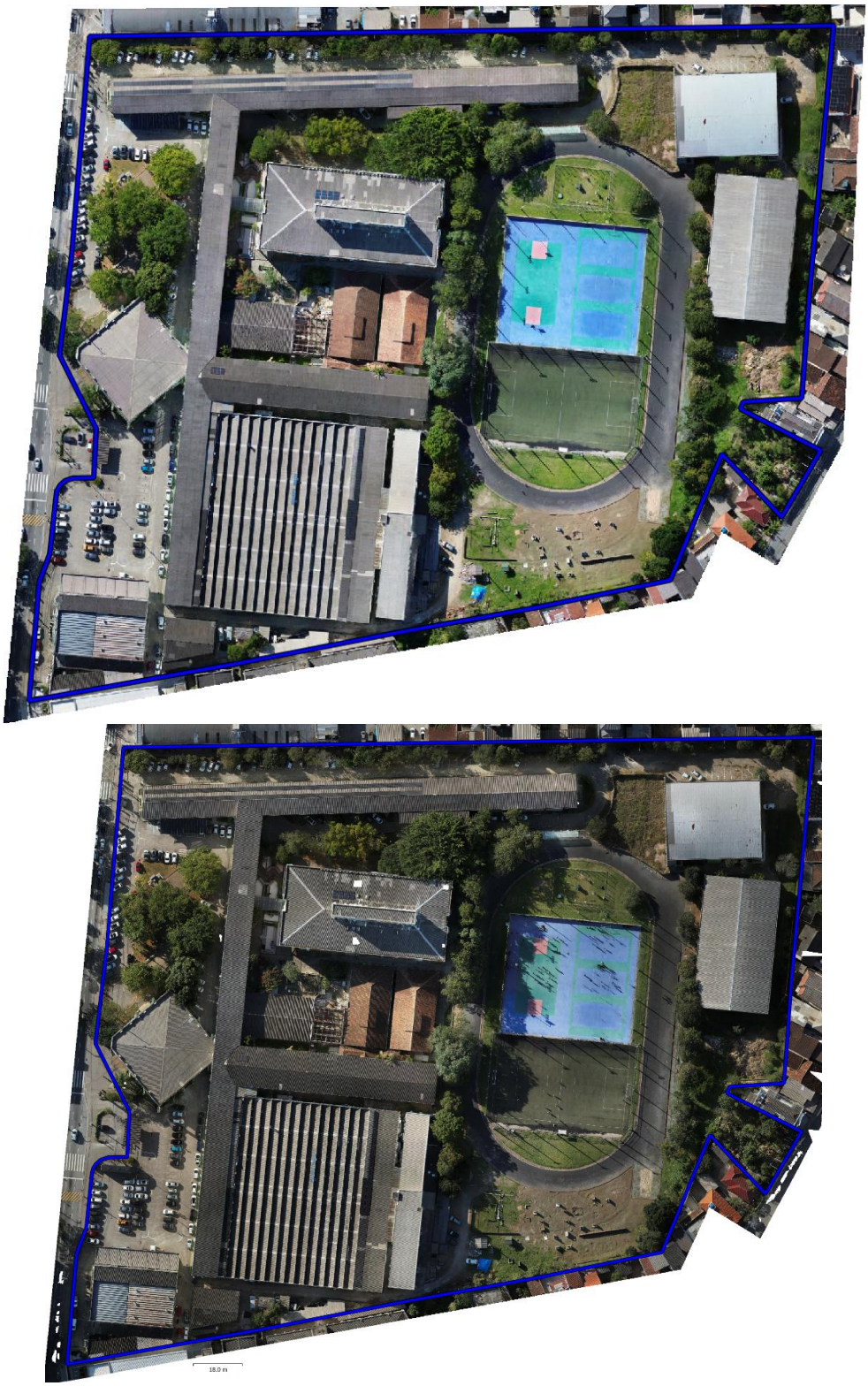

Figure 6. Orthomosaic generated with the Mini 3 (top) and Matrice 350 + P1 (bottom).

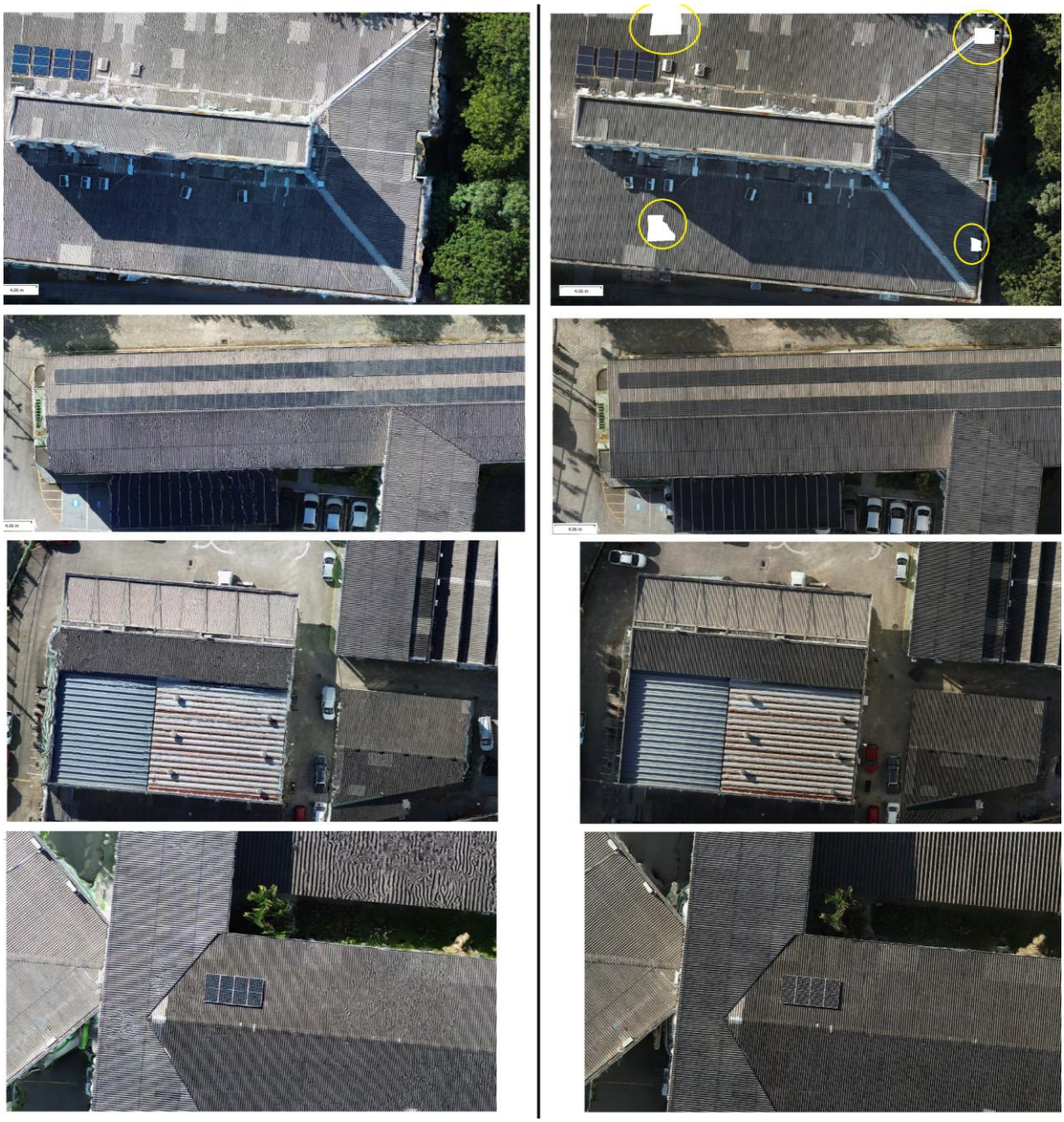

Figure 7. Close-up comparisons of orthomosaic details: Mini 3 (left) and Matrice 350 + P1 (right), highlighting residual artifacts and edge distortions.

4.2 Accuracy

The first assessment of georeferencing accuracy was performed within the photogrammetric software, which provides the three-dimensional root mean square error (RMS) for control and check points. Table 4 summarizes these results. The Mini 3 dataset exhibited a 3D RMS of approximately 10 cm, while the Matrice 350 + P1 achieved around 4 cm. These values reflect the internal network adjustment and include multiple measurements of each ground control point, ranging from four to eleven images per point. The higher number of image observations

combined with the superior image quality of the Matrice can explain its consistently lower residuals.

Table 4. RMS values from Metashape

Metashape - RMS (cm)							
UAS	**Point type**	**Number**	**XEasting**	**Y/Northing**	**Z/Altitude**	**XY**	**Total**
Mini 3	Control	11	1.78	2.10	1.73	2.76	3.25
	Check	27	4.05	3.54	8.56	5.38	10.11
Matrice	Check	27	1.43	1.89	3.16	2.37	3.95

A second evaluation focused on the final photogrammetric products, in which the geodetic coordinates of the check points were extracted directly from the orthomosaics and digital surface models and subsequently analyzed using the GeoPEC software. This external validation provides an independent measure of positional accuracy, isolating the results from the internal bundle adjustment. Table 5 lists the reference geodetic coordinates along with the positional discrepancies for each check point measured in the orthomosaics.

Table 5. Reference geodetic coordinates and positional discrepancies (Δ) of check points measured in the orthomosaics (UTM Zone 22S).

ID	Reference			Mini 3			Matrice 350 + P1		
	East (m)	North (m)	Alt.(m)	Δ East (m)	Δ North (m)	Δ Alt. (m)	Δ East (m)	Δ North (m)	Δ Alt. (m)
3	742642,639	6945292,429	13,367	0,02	0,06	-0,03	0,01	0,00	-0,02
4	742644,821	6945303,168	13,765	0,01	0,01	0,03	-0,01	-0,04	-0,01
5	742635,965	6945327,000	13,214	0,03	0,04	0,05	0,02	0,00	-0,02
10	742675,487	6945348,377	13,277	0,05	0,03	0,01	0,02	-0,01	-0,04
19	742742,762	6945403,823	13,794	0,07	0,00	0,02	0,02	-0,01	-0,02
20	742735,659	6945434,980	13,552	0,05	0,03	0,06	0,02	0,01	-0,02
22	742715,080	6945471,025	13,118	0,03	-0,04	-0,09	0,02	0,02	-0,04
23	742661,567	6945472,481	11,37	-0,06	-0,06	-0,30	-0,01	0,02	-0,09
26	742666,436	6945439,342	13,155	-0,05	-0,03	-0,01	0,00	0,00	-0,03
27	742695,646	6945431,846	13,228	-0,05	-0,02	-0,05	-0,02	0,01	-0,05
30	742664,211	6945378,280	13,563	0,01	0,03	0,07	0,01	0,02	-0,02
32	742645,500	6945410,973	13,39	-0,01	0,01	0,05	-0,02	0,03	-0,04
35	742536,379	6945443,923	10,859	-0,01	-0,02	0,06	0,00	0,03	0,00
38	742503,348	6945437,288	10,896	0,00	-0,01	0,11	-0,01	0,03	-0,01
39	742501,520	6945390,785	10,85	-0,06	-0,03	0,09	-0,02	-0,02	0,00
45	742496,125	6945339,448	10,442	-0,02	0,01	0,11	-0,01	-0,01	-0,02
47	742524,014	6945347,198	10,781	-0,05	0,00	0,06	0,00	0,00	-0,04
48	742526,548	6945321,463	10,869	-0,03	0,01	0,04	-0,01	-0,02	-0,01
49	742522,923	6945302,498	10,818	-0,04	0,02	0,01	0,00	-0,03	-0,03
55	742486,433	6945290,201	10,648	-0,05	0,04	0,10	-0,03	-0,02	-0,02
57	742523,374	6945275,004	10,822	-0,03	0,04	-0,09	0,01	-0,03	-0,05
59	742584,922	6945277,828	11,296	-0,03	0,05	-0,13	0,02	-0,01	-0,03
62	742627,326	6945304,113	13,777	-0,01	0,02	0,25	0,00	0,00	-0,02
64	742628,513	6945320,911	13,178	0,00	0,01	0,08	0,02	-0,01	-0,02
65	742618,366	6945306,927	13,057	-0,06	0,04	0,02	-0,02	0,00	-0,02
67	742655,885	6945326,574	13,064	-0,01	0,05	-0,01	0,01	-0,01	-0,05
69	742698,877	6945365,224	13,167	0,02	0,00	-0,03	0,00	-0,01	-0,05

The GeoPEC analysis yielded an overall RMS of approximately 11 cm for the Mini 3 orthomosaic and 4 cm for the Matrice dataset, confirming the superior positional consistency of the professional platform (Table 6).

Table 6. RMS values from GeoPEC

Geopec - RMS (cm)							
UAS	**Point type**	**Number**	**X/Easting**	**Y/Northing**	**Z/Altitude**	**XY**	**Total**
Mini 3	Check	27	3.77	3.17	9.86	4.93	11.02
Matrice	Check	27	1.36	1.84	3.39	2.30	4.09

The positional accuracy of both orthomosaics was further classified according to the Brazilian Cartographic Accuracy Standard (PEC – Decree-Law 89.817/1984) and the INCRA Georeferencing Standard for Rural Properties. Based on the GeoPEC analysis, the Mini 3 achieved planar RMS of about 5 cm and vertical RMS of 9 cm, whereas the Matrice orthomosaic reached approximately 2 cm (planar) and 3 cm (vertical). Despite the pronounced advantage of the Matrice, both products meet PEC Class A requirements for the 1:1000 scale and comply with INCRA limits for artificial boundaries ($\leqslant$ 0.5 m), ensuring their suitability for precise 2D area calculations and other cadastral applications.

5. CONCLUSIONS AND FUTURE WORK

This study presented a comparative evaluation of orthomosaics and digital surface models generated by a low-cost UAS (DJI Mini 3) and a professional-grade platform (DJI Matrice 350 RTK + P1 camera) for urban cadastre applications.

The results demonstrated the clear superiority of the Matrice 350 RTK + P1, which, operated with direct georeferencing (Network RTK), achieved a ground sampling distance (GSD) of 0.84 cm and a final positional RMS of 4.09 cm, while delivering smoother DSM surfaces and sharper building edges. These qualities are particularly valuable for 3D modeling, volumetric analysis, and high-precision cadastral surveys. However, this performance comes at the cost of significantly higher equipment price and longer processing times (4 h 47 min versus 32 min for the Mini 3). The DJI Mini 3, on the other hand, despite its lower image resolution, higher RMS ($\approx$11 cm), and noisier DSM, proved capable of meeting the PEC Class A requirements for 1:1000 mapping when processed with indirect georeferencing supported by dense ground control. Its sub-250 g weight exempts it from flight authorization in Brazil, simplifying field operations. The Mini's portability, ease of deployment, and reduced acquisition cost make it a compelling alternative for small municipalities or institutions facing budget constraints, provided users accept the greater need for manual corrections and a more labor-intensive workflow during post-processing.

It is important to emphasize that only a single nadir flight plan was employed in this experiment, without cross-flight patterns or oblique imagery. Incorporating 90° + 45° image combinations or cross-flight designs would likely improve model precision and reduce noise, especially in areas with complex roof geometries. Furthermore, although the Matrice

produced higher-quality DSMs, both datasets would benefit from additional post-processing to remove artifacts before generating final cartographic products.
Future research should conduct a comprehensive cost–benefit analysis comparing the economic trade-offs between establishing and measuring GCPs for indirect georeferencing and investing in professional systems with high-precision GNSS/IMU hardware for direct georeferencing. Studies should also investigate the effects of cross-flight missions, oblique image acquisition, and automated noise filtering on the accuracy and efficiency of low-cost UAS photogrammetry. Such analyses will help guide municipalities and public institutions in balancing budget limitations, operational complexity, and accuracy demands when selecting UAS technology for cadastral and urban mapping projects.

REFERENCES

Blázquez, M., Colomina, I., 2012. Relative INS/GNSS aerial control in integrated sensor orientation: Models and performance. ISPRS J. Photogramm. Remote Sens. 67, 120–133. https://doi.org/10.1016/j.isprsjprs.2011.11.003

Cledat, E., Cucci, D.A., Skaloud, J., 2020. Camera Calibration Models and Methods for Corridor Mapping with Uavs. ISPRS Ann. Photogramm. Remote Sens. Spat. Inf. Sci. 5, 231–238. https://doi.org/10.5194/isprs-annals-V-1-2020-231-2020

Defesa, M. Da, Brasileiro, E., Tecnologia, D.D.C.E., 2016. Controle de Qualidade de Dados Geoespaciais (ET-CQDG).

Galo, M., Camargo, P. de O., 1994. Utilização do GPS no controle de qualidade de cartas. I Congr. Bras. Cadastro Técnico Multifinalitário 41–48. https://doi.org/10.13140/RG.2.1.1790.1603
Geopec, n.d. GeoPEC - Software para avaliação da acurácia posicional em dados cartográficos.

IBGE, n.d. Rede Brasileira de Monitoramento Contínuo dos Sistemas GNSS [WWW Document]. URL https://www.ibge.gov.br/geociencias-novoportal/informacoes-sobre-posicionamento-geodesico/rede-geodesica/16258-rede-brasileira-de-monitoramento-continuo-dos-sistemas-gnss-rbmc.html?=&t=o-que-e (accessed 2.24.19).

INCRA, 2022. Manual Técnico para o Georreferenciamento de Imóveis Rurais – 2ª Edição.
Jiménez-Martínez, M.J., Farjas-Abadia, M., Quesada-Olmo, N., 2021. An Approach to Improving GNSS Positioning Accuracy Using Several GNSS Devices. Remote Sens. 2021, Vol. 13, Page 1149 13, 1149. https://doi.org/10.3390/RS13061149

Leick, A., Rapoport, L., Tatarnikov, D., 2015. GPS SATELLITE SURVEYING, Fourth. ed, John Wiley & Sons, Inc. American Congress on Surveying & Mapping, New Jersey. https://doi.org/10.16309/j.cnki.issn.1007-1776.2003.03.004
Merchant, D.C., 1982. Spatial Accuracy Standards for Large Scale Line Maps, in: In Proceedings of the Technical Congress on Surveying and Mapping.

Mikhail, E.M., Bethel, J.S., McGlone, J.C., 2001. Introduction to modern photogrammetry, Volume 1 479.

Sanz-Ablanedo, E., Chandler, J.H., Rodríguez-Pérez, J.R., Ordóñez, C., 2018. Accuracy of Unmanned Aerial Vehicle (UAV) and SfM photogrammetry survey as a function of the number and location of ground control points used. Remote Sens. 10. https://doi.org/10.3390/rs10101606

Štroner, M., Urban, R., Seidl, J., Reindl, T., Brouček, J., 2021. Photogrammetry using UAV-mounted GNSS RTK: Georeferencing strategies without GCPs. Remote Sens. 13. https://doi.org/10.3390/rs13071336

BIOGRAPHICAL NOTES

Allan Gomes: Professor, Academic Department of Civil Construction (DACC), IFSC
Renato Zetehaku Araujo: Professor, Academic Department of Civil Construction (DACC), IFSC.

Francisco Henrique de Oliveira: Professor, Department of Geography (FAED), UDESC.

CONTACTS

Allan Gomes
Instituto Federal de Santa Catarina - IFSC
Address: Av. Mauro Ramos, 950 - Centro, Florianópolis - SC, 88010-400
Florianópolis
BRAZIL
Phone: + 55 48 3211-6061
E-mail: allan.gomes@ifsc.edu.br

Renato Zetehaku Araujo
Instituto Federal de Santa Catarina - IFSC
Address: Av. Mauro Ramos, 950 - Centro, Florianópolis - SC, 88010-400
Florianópolis
BRAZIL
Phone: + 55 48 3211-6061
E-mail: renato.araujo@ifsc.edu.br

Francisco Henrique de Oliveira
Universidade do Estado de Santa Catarina (UDESC)
Florianópolis, SC
BRAZIL
Phone: +5548984113384
E-mail: francisco.oliveira@udesc.br